

### III. Ion Channel Expression in PMA-differentiated Human THP-1 Macrophages

T.E. DeCoursey<sup>1</sup>, S.Y. Kim<sup>2</sup>, M.R. Silver<sup>2</sup>, F.N. Quandt<sup>1,3</sup>

<sup>1</sup>Department of Molecular Biophysics and Physiology,

<sup>2</sup>Department of Medicine, Pulmonary Division,

<sup>3</sup>Multiple Sclerosis Center, Rush Presbyterian St. Luke's Medical Center, 1653 West Congress Parkway Chicago, IL 60612

Received: 19 September 1995/Revised: 14 March 1996

**Abstract.** Ion channel expression was studied in THP-1 human monocytic leukemia cells induced to differentiate into macrophage-like cells by exposure to the phorbol ester, phorbol 12-myristate 13-acetate (PMA). Inactivating delayed rectifier K<sup>+</sup> currents,  $I_{DR}$ , present in almost all undifferentiated THP-1 monocytes, were absent from PMA-differentiated macrophages. Two K<sup>+</sup> channels were observed in THP-1 cells only after differentiation into macrophages, an inwardly rectifying K<sup>+</sup> channel ( $I_{IR}$ ) and a Ca<sup>2+</sup>-activated maxi-K channel ( $I_{BK}$ ).  $I_{IR}$  was a classical inward rectifier, conducting large inward currents negative to  $E_K$  and very small outward currents.  $I_{IR}$  was blocked in a voltage-dependent manner by Cs<sup>+</sup>, Na<sup>+</sup>, and Ba<sup>2+</sup>, block increasing with hyperpolarization. Block by Na<sup>+</sup> and Ba<sup>2+</sup> was time-dependent, whereas Cs<sup>+</sup> block was too fast to resolve. Rb<sup>+</sup> was sparingly permeant. In cell-attached patches with high [K<sup>+</sup>] in the pipette, the single  $I_{IR}$  channel conductance was ~30 pS and no outward current could be detected.  $I_{BK}$  channels were observed in cell-attached or inside-out patches and in whole-cell configuration. In cell-attached patches the conductance was ~200–250 pS and at potentials positive to ~100 mV a negative slope conductance of the unitary current was observed, suggesting block by intracellular Na<sup>+</sup>.  $I_{BK}$  was activated at large positive potentials in cell-attached patches; in inside-out patches the voltage-activation relationship was shifted to more negative potentials by increased [Ca<sup>2+</sup>]. Macroscopic  $I_{BK}$  was blocked by external TEA<sup>+</sup> with half block at 0.35 mM. THP-1 cells were found to contain mRNA for Kv1.3 and IRK1. Levels of mRNA coding for these K<sup>+</sup> channels were studied by competitive PCR (polymerase chain reaction), and were found to change upon differentiation in

the same direction as did channel expression: IRK1 mRNA increased at least 5-fold, and Kv1.3 mRNA decreased on average 7-fold. Possible functional correlates of the changes in ion channel expression during differentiation of THP-1 cells are discussed.

**Key words:** Macrophage — Ion channels — K<sup>+</sup> channels — IRK1 — Kv1.3 — Cellular differentiation

#### Introduction

As monocytes differentiate into mature, nondividing macrophages they become capable of a large variety of responses, including chemotaxis, phagocytosis, and secretion of numerous cytokines and other substances. The expression of membrane proteins changes during differentiation, in some cases dramatically. Here we explore changes in ion channel expression in the human leukemia cell line, THP-1, after differentiation induced by PMA. Our long-term goals include defining channels as markers for stages of differentiation, evaluating the mechanisms by which channel expression is regulated, and exploring possible functional correlates of different patterns of ion channel expression. A large body of literature exists describing ion channel expression in various monocytes and related cell lines (Gallin, 1991). One advantage of using the THP-1 cell line over primary human monocytes is a more uniform cell population—macrophages which differentiate terminally in different tissues have very different properties (e.g., Peters-Golden et al., 1990), including divergent ion channel expression (Nelson, Jow & Popovich, 1990b). THP-1 cells are more differentiated than many other monocytic cell lines (Hass et al., 1990; Auwerx, 1991) and are committed to the macrophage lineage. In contrast, the more

primitive HL-60 or ML-1 cells can be induced to differentiate along either macrophage or granulocytic pathways. Compared in detail with other cell lines, the THP-1 model more closely resembles the differentiation of human monocytes (Auwerx, 1991).

Although four of the seven or more types of ion channels in THP-1 cells were present both before and after differentiation, the expression of three K<sup>+</sup> channels changed dramatically, apparently in an all-or-none manner under the conditions of these studies. Inactivating delayed rectifier K<sup>+</sup> currents,  $I_{DR}$ , were present in most control THP-1 monocytes (Kim, Silver & DeCoursey, 1996), but absent in differentiated cells; "maxi-K" Ca<sup>2+</sup>-activated K<sup>+</sup> channels ( $I_{BK}$ ) and inward rectifier K<sup>+</sup> currents ( $I_{IR}$ ) were absent from undifferentiated monocytes, but present in many differentiated THP-1 macrophages. We identify the molecular species evidently responsible for  $I_{DR}$  and  $I_{IR}$  in THP-1 cells by the polymerase chain reaction (PCR), and explore the hypothesis that changes in the expression of these K<sup>+</sup> channels are mediated by changes in the levels of channel-specific mRNA. The observed correlation between mRNA levels and K<sup>+</sup> channel expression provides a powerful tool for future studies of mechanisms of regulation of ion channel expression.

## Materials and Methods

### CELL PREPARATION

THP-1 cells were cultured as described (Kim et al., 1996). To induce differentiation, cells were incubated with 10 ng/ml PMA (Sigma Chemical Company, St. Louis, MO) for three days in 35-mm tissue culture dishes containing several small pieces of sterile glass coverslips. One manifestation of differentiation is adherence; cells adhering to the coverslip fragments were transferred to the recording chamber. Some cells were studied immediately, others were washed with HBSS (Hanks Balanced Salt Solution) or with RPMI to remove the PMA and then cultured in PMA-free media another 1 or 2 days before use in patch clamp experiments. No qualitative differences were observed between cells studied immediately after PMA treatment and those studied one or two days later; evidently the dramatic changes in K<sup>+</sup> channel expression were not reversed rapidly. Differentiation of THP-1 and other myeloid leukemia cell lines is not permanent; retrodifferentiation occurs after 3-4 weeks, with complete reversion of all morphological and biochemical changes (Hass, 1992).

### ELECTROPHYSIOLOGY

Methods and solutions are described in a companion paper (Kim et al., 1996).

### Estimating $P_{open}$ for $I_{BK}$ Channels

The total number of  $I_{BK}$  channels present in membrane patches,  $N$ , was estimated in several ways. In patches with only a few channels, all

channels were open simultaneously often enough to establish directly the maximum number of channels. When more channels were present, current amplitude histograms were constructed, and the probability of each number,  $r$ , of simultaneously open channels,  $P(r)$ , measured by integrating under the appropriate peak. Assuming a binomial distribution:

$$P(r) = N!/(r!(N-r)!) (P_{open})^r (1 - P_{open})^{(N-r)} \quad r = 0, 1, \dots, N \quad (1)$$

(p. 163, Colquhoun & Hawkes, 1985) which is valid if the channels are identical and independent, we assumed several guesses of  $N$  and compared calculated  $P(r)$  distributions with the actual  $P(r)$  data to select the optimal value of  $N$ . When more than a dozen channels were present, a lower limit for  $N$  was obtained by dividing the maximum observed K<sup>+</sup> current at the most positive potential studied (usually RP + 190 mV, that is, 190 mV positive to the resting potential) by the unitary current at that potential. The error in these estimates increases with  $N$  and may be substantial at large  $N$ . In cell-attached patches, the total number of channels in the patch often was not well determined, because [Ca<sup>2+</sup>]<sub>i</sub> was at physiological levels, and at the most positive potentials tested  $P_{open}$  appeared to be only ~0.5. In inside-out patches in which  $N$  was known (e.g., Fig. 8),  $P_{open}$  could be calculated directly, and the observed distribution fit the binomial prediction well, supporting the independence of channel opening.

## MOLECULAR BIOLOGY

### Isolation of RNA

Prior to amplification of cDNA, total RNA was isolated using TRIZOL reagent (Bethesda Research Labs, Gaithersburg, MD) according to the manufacturer's procedures. This is a modification of the acid-guanidinium-phenol extraction method of Chomczynski (1993). The concentration of RNA in any sample was measured by spectrophotometry. Samples were stored at -70°C until used for reverse transcription.

### Reverse Transcription-PCR

Reverse transcription (RT) was carried out using Superscript reverse transcriptase (Bethesda Research Labs). Each RT reaction was normalized by adding a constant 1  $\mu$ g of RNA per 20  $\mu$ l reaction volume. The resulting cDNA was amplified using one of three primer sets. To amplify human IRK1 cDNA, the upstream (sense strand) primer was 5'-ACAGGACATTGACAACGCAG. The downstream IRK1 primer sequence was 5'-GCGTGTCCGTACTAGTGCTT. To amplify Kv1.3 cDNA, the upstream primer was 5'-ATCTTCAAGCTGTCGCCA and the downstream primer 5'-CGATCACCATATACTCCGAC. We also amplified glyceraldehyde-3-phosphate dehydrogenase (G3PDH) cDNA (Ercolani et al., 1988) in some control experiments using primers having the upstream sequence 5'-TGATGACATCAAGAAGGTGGTGAAG and downstream sequence 5'-TCCTGGAGGCCATGTAGGCCAT.

### Sequencing

The cDNA amplified by PCR was partially sequenced by a thermocycle sequencing procedure which uses dideoxynucleotides for termination of extension. The primer was biotinylated, and a colorimetric reaction employing the biotin complexed with streptavidin and alkaline

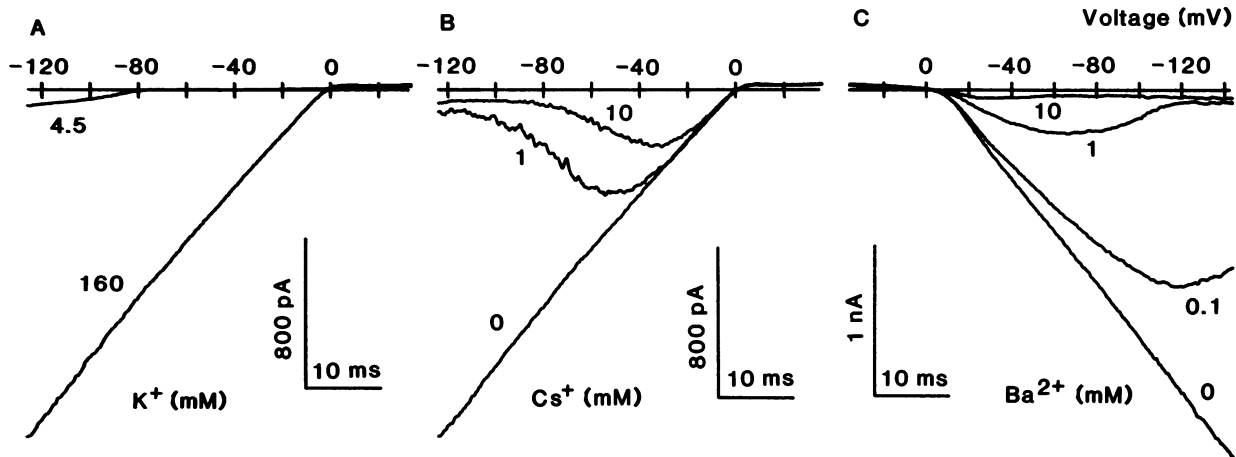


**Fig. 1.** (A)  $[K^+]_o$  dependence of  $I_{IR}$ . Voltage ramps were applied in Ringer's solution (4.5 mM  $K^+$ ) and then in isotonic  $K^+$  Ringer's solution (160 mM  $[K^+]_o$ ) from  $V_{hold} = 0$  mV. Pipette contained  $Mg^{2+}$ -free KMeSO<sub>3</sub>, filter 2 kHz. (B) Voltage-dependent block of  $I_{IR}$  by  $Cs^+$  in symmetrical high  $[K^+]$  in the same cell. Because  $Cs^+$  block is very rapid, the voltage dependence of block is reasonably accurately defined by currents during voltage ramps. The indicated concentration of  $CsCl$  was added to  $K^+$  Ringer's solution. (C) Voltage-dependent block of  $I_{IR}$  by  $Ba^{2+}$  in symmetrical high  $[K^+]$ , also in the same cell.  $Ba^{2+}$  block is relatively slow; thus the level of block at any given voltage during downward voltage ramps will underestimate the true steady-state level. During up ramps like those in A or B voltage-dependent block was obscured because block was substantial at large negative potentials, and the ramp was too rapid to allow  $I_{IR}$  channels to become unblocked.

phosphatase then detected the strands after blotting of the sequencing gel.

### Competitive PCR

The competitive PCR procedure was employed to assay quantitatively the amount of cDNA in the RT reaction (see Gilliland et al., 1990). A volume of the RT reaction was amplified with the primers for one channel, in the presence of a DNA fragment which competes for the same primers. An increasing concentration of competitor DNA was added to aliquots of any RT reaction. Following PCR, the ratio of amplified competitor to amplified channel DNA was used to determine the original amount of cDNA. The competitor was constructed by appending the channel primer sequences onto a DNA fragment (PCR Mimic™ Construction Kit, Clontech, Palo Alto, CA) via PCR. The length of the competitor was made to be larger than the channel DNA. The concentration of competitor stock was measured by spectrophotometry or by gel electrophoresis.

The products of the PCR reaction were subjected to electrophoresis. The relative ratios of channel to competitor DNA amplified by PCR were determined by measuring the ratio of the intensity of fluorescence of the two bands in any lane, after staining with ethidium bromide. To measure the intensity, an image taken with a CCD camera was analyzed by computer-aided densitometry. To determine the intensity, background was first subtracted, and the amplitude of each pixel of the image was integrated over a fixed area of the gel.

## Results

### ION CHANNELS FOUND ONLY IN DIFFERENTIATED THP-1 CELLS

#### Inwardly Rectifying $K^+$ Current ( $I_{IR}$ )

PMA-treated cells expressed an inwardly rectifying  $K^+$  current ( $I_{IR}$ ) resembling that in other macrophage-related

cells (Gallin, 1991). Figure 1 illustrates  $I_{IR}$  currents during voltage ramps. In Ringer's solution with 4.5 mM extracellular  $K^+$ ,  $[K^+]_o$ , inward currents were apparent at membrane potentials negative to -80 mV. When the bathing solution was changed to 160 mM  $K^+$  Ringer's solution, the inward currents were much larger and were evident negative to 0 mV. Outward currents in either solution were quite small, and the small bump of outward current visible in  $K^+$  Ringer's decreased with depolarization, resulting in a region of negative slope conductance. The  $[K^+]_o$  dependence and strong inward rectification is typical of inward rectifier  $K^+$  currents in many cells.

Inward rectifier channels are blocked by several extracellular cations. Figure 1B illustrates that  $Cs^+$  produced potent voltage-dependent block. Block by 1 mM  $Cs^+$  was almost complete at -120 mV, and was relieved by depolarization, with almost no block at -30 mV. Increasing  $Cs^+$  to 10 mM increased block at all potentials and shifted the block to more positive potentials. Block by  $Ba^{2+}$  was also voltage dependent, as illustrated in Fig. 1C. In this experiment the voltage was ramped from positive to negative. Even 0.1 mM  $Ba^{2+}$  produced distinct block, which was markedly enhanced at more negative potentials. More profound block was seen at 1 mM  $Ba^{2+}$ , and at 10 mM  $Ba^{2+}$  block was nearly complete, although a small inward current dip is still present. When the voltage was ramped from negative to positive,  $Ba^{2+}$  block appeared to be deeper and little voltage-dependence was observed. This behavior reflects the relatively slow time-dependence of  $Ba^{2+}$  block; the deep block at negative potentials was not relieved by depolar-

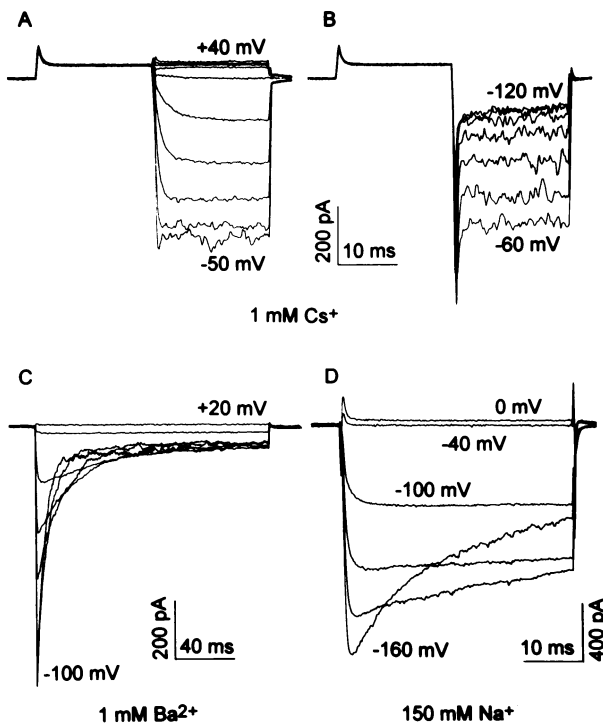


**Fig. 2.** Voltage-dependent block of  $I_{IR}$  by cations. (A and B) Block of  $I_{IR}$  by  $Cs^+$  is rapid and strongly voltage-dependent. A cell in  $K^+$  Ringer's solution with 1 mM  $Cs^+$  was held at 0 mV and a 20 msec prepulse applied to +20 mV to "close" the channels and remove any residual block at  $V_{hold} = 0$  mV. A series of test pulses was applied, ranging from +40 to -120 mV in -10 mV increments. The currents during pulses from +40 to -50 mV are superimposed in A, and the currents for pulses to -60 through -120 mV are plotted in B. The strong inward rectification of this conductance is apparent. During small hyperpolarizing pulses the time-dependent activation of  $I_{IR}$  can be seen. By -40 mV the inward currents are quite noisy, and at potentials negative to -50 mV the currents become smaller, as  $Cs^+$  block is enhanced by hyperpolarization. The onset of block is too fast to be resolved convincingly. The pipette contained divalent-free KMeSO<sub>3</sub> solution, filter 2 kHz. (C) Block of  $I_{IR}$  by 1 mM  $Ba^{2+}$  in  $K^+$  Ringer's solution in the same cell is slower and strongly voltage-dependent. Illustrated currents are in 20 mV increments between +20 and -100 mV.  $V_{hold}$  was +10 mV, filter 2 kHz. (D) Voltage- and time-dependent decay of  $I_{IR}$  in normal Ringer's solution in a different cell. Illustrated currents at 0 and -40 mV show a small leak current, and the currents at -100 through -160 mV in -20 mV increments show the increasingly rapid and complete block, presumably by the 160 mM  $Na^+$ .  $V_{hold}$  was -60 mV, filter 2 kHz.

ization as fast as the voltage was ramped (see also below).

Block by  $Cs^+$  on the other hand appeared similar whether the voltage was ramped up or down. This can be explained if  $Cs^+$  block is rapid, and  $Ba^{2+}$  block is slow. Figure 2 confirms this explanation. Figures 2A and B illustrate a family of currents during voltage pulses applied to a cell studied in the presence of 1 mM  $Cs^+$  added to  $K^+$  Ringer's, after a depolarizing prepulse intended to remove any block and to "close" the channels. Very little current was observed at positive potentials.

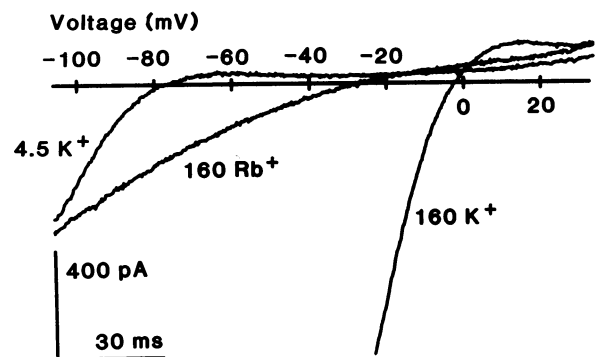


**Fig. 3.** Whole-cell  $I_{IR}$  currents during voltage ramps, in Ringer's solution (4.5 mM  $[K^+]_o$ ), and 160 mM  $Rb^+$  or  $K^+$  Ringer's solution. In  $Rb^+$  Ringer's solution there is distinct inward current, blockable by  $Ba^{2+}$  (not shown), indicating that  $Rb^+$  can carry small inward currents through  $I_{IR}$  channels.  $V_{rev}$ , measured without leak correction, shifted 25 mV more negative in  $Rb^+$  than in  $K^+$  Ringer's.  $V_{hold} = -80$  mV, pipette KMeSO<sub>3</sub>.

At small negative potentials large inward currents turned on with a time constant of several msec. This time-dependent turn-on is another hallmark of  $I_{IR}$  currents, and was seen in the absence of  $Cs^+$  as well. At -40 mV the inward current in Fig. 2A became much noisier, and with further hyperpolarization beyond -50 mV its amplitude decreased (Fig. 2B), both features reflecting  $Cs^+$  block. The decay of inward current during large hyperpolarizing pulses was rapid and complete in <2 msec, and could not be distinguished reliably from a capacity transient. Clearly,  $Cs^+$  block is very rapid.

Figure 2C illustrates the distinctive time dependence of the voltage-dependent block by 1 mM  $Ba^{2+}$ . The inward current was large at first and decayed slowly at -20 mV and more rapidly and completely at more negative potentials. Under these conditions in the absence of  $Ba^{2+}$  little decay of inward current was observed. Voltage- and time-dependent block by  $Ba^{2+}$  is another classical property of true inward rectifiers, including  $I_{IR}$  in murine J774.1 macrophages (McKinney & Gallin, 1988).

In Ringer's solution,  $I_{IR}$  decayed with time during large hyperpolarizing pulses, the rate and extent of decay increasing with hyperpolarization (Fig. 2D). When all  $Na^+$  was replaced by  $NMG^+$ , this decay disappeared. The decay reflects time- and voltage-dependent block by  $Na^+$ , as has been described for  $I_{IR}$  in many tissues (Ohmori, 1978; Standen & Stanfield, 1979; Biermans, Vereecke & Carmeliet, 1987; Harvey & Ten Eick, 1989).

$Rb^+$  is a weakly permeant blocker of inward rectifier channels (Hutter & Williams, 1979; Standen & Stanfield, 1980; Silver, Shapiro & DeCoursey, 1994). Whole-cell ramp currents are illustrated in Fig. 3 for a cell in Ringer's and  $K^+$  Ringer's solutions. The voltage range of channel activation shifted along with  $E_K$  and small outward currents were present just positive to  $E_K$  both in Ringer's and  $K^+$  Ringer's solutions, as was shown in Fig.

1A. When  $K^+$  Ringer's solution was replaced with  $Rb^+$ , small inward currents persisted, and  $V_{rev}$  shifted  $\sim 25$  mV more negative. As in skeletal muscle (Standen & Standen, 1980) and endothelial cells (Silver et al., 1994),  $I_{IR}$  in THP-1 cells has a relative permeability to  $Rb^+$  about 0.4 that of  $K^+$ , calculated with the Goldman-Hodgkin-Katz voltage equation, but a relative conductance  $< 10\%$  that of  $K^+$ .

### Single $I_{IR}$ Channels

Single  $I_{IR}$  channels could be identified in cell-attached patches by the absence of outward current and high open probability at potentials negative to  $E_K$ . The average leak-subtracted single open channel current-voltage relationship is plotted in Fig. 4 for a patch containing one active  $I_{IR}$  channel. The slope conductance was 30–35 pS, similar to that of  $I_{IR}$  channels in J774.1 cells (McKinney & Gallin, 1988). The inside-out patch configuration allowed exploration of the effects of intracellular divalent cations on the  $I_{IR}$  channel. Little difference in either current amplitude or open probability was detected after 5 min exposure to KMeSO<sub>3</sub> solutions containing 1.9 mM Mg<sup>2+</sup>, 10  $\mu$ M Ca<sup>2+</sup>, or a nominally divalent-free solution. Apparently the  $I_{IR}$  channel is neither activated by Ca<sup>2+</sup> nor is its rectification (as observed in voltage ramps) the result of block by Mg<sup>2+</sup>.

### LARGE CONDUCTANCE Ca<sup>2+</sup>-ACTIVATED K<sup>+</sup> CURRENT ( $I_{BK}$ )

Large-conductance, voltage- and calcium-activated "maxi-K" or  $I_{BK}$  channels were observed in cell-attached or excised inside-out patches, and in whole-cell currents.

In cell-attached patches,  $I_{BK}$  channels could be identified by their large unitary conductance, activation only at extreme positive potentials, and by a characteristic negative conductance region at voltages positive to about +100 mV. To facilitate recording  $I_{BK}$  channels, we routinely ramped the voltage rapidly from large positive toward negative potentials, so that any open channel would tend to remain open for some time before closing. Figure 5A illustrates a single leak-subtracted ramp current in which one  $I_{BK}$  channel remained open to about -20 mV. The maximum slope conductance was 220 pS, and in the negative slope conductance region the open-channel noise was clearly increased. This negative conductance region was observed in all  $I_{BK}$  channels in cell-attached patches, and is reminiscent of the voltage-dependent block of  $I_{BK}$  outward current by cytoplasmic Na<sup>+</sup> (Marty, 1983).

The average open-channel current-voltage relationship for the  $I_{BK}$  channel in Fig. 5A is plotted in Fig. 5B. The  $I$ - $V$  relation is sublinear (i.e., the slope conductance decreases) at large negative potentials as well as at large

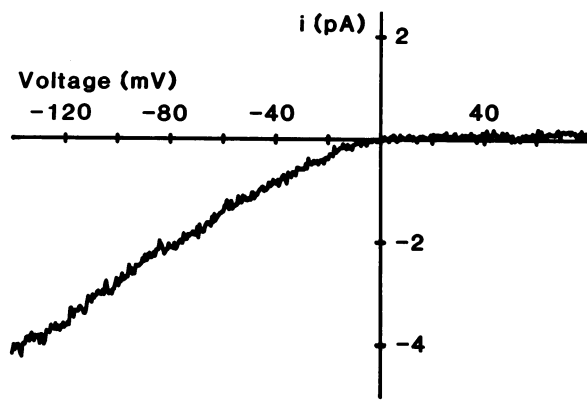


**Fig. 4.** Single  $I_{IR}$  channel current-voltage relationship in an inside-out patch, containing one active  $I_{IR}$  channel. The slope conductance measured between -140 and -40 mV was 34 pS, measured closer to  $V_{rev}$  the conductance was 31 pS. Averaged closed-channel records were subtracted from averaged open-channel records. Because no distinct openings were detected at potentials positive to  $V_{rev}$ , records in which the  $I_{IR}$  channel appeared to be open over the entire voltage range negative to  $V_{rev}$  were included in the "open" average. Pipette solution 3  $\mu$ M Ca<sup>2+</sup> KMeSO<sub>3</sub>, bath solution Mg-free KMeSO<sub>3</sub>. The unitary conductance, the high  $P_{open}$  at negative potentials and absence of detectable openings positive to  $V_{rev}$  were indistinguishable in this patch when exposed to 1.9 mM Mg<sup>2+</sup> or 10  $\mu$ M Ca<sup>2+</sup> KMeSO<sub>3</sub> solutions (each for 5 min) from the behavior in divalent-free KMeSO<sub>3</sub> solution. The voltage was ramped from -140 to +80 mV at 0.88 V/sec, filter 1 kHz.

positive potentials. Similar sublinearity has been attributed to diffusion limitation in the approach of K<sup>+</sup> to the  $I_{BK}$  channel mouth (Yellen, 1984). Diffusion limitation may contribute at positive potentials as well, but could not cause negative conductance.

The voltage dependence of  $I_{BK}$  opening can be seen in the cell-attached patch experiment illustrated in Fig. 6. Two brief channel openings can be seen at +40 mV. At +80 mV up to 5 channels were open simultaneously, and all channels were closed only infrequently. By +120 mV many channels were open throughout the pulse. At large positive potentials the individual current levels are hard to distinguish, partly because the number of open channels was large, but partly because of the increased open-channel noise (cf. Fig. 5A). Clearly the probability of the  $I_{BK}$  channel being open,  $P_{open}$ , is voltage dependent.  $I_{BK}$  events were detected in most patches at +60 mV although  $P_{open}$  was small, and at +40 mV with even lower  $P_{open}$ . Thus in intact cells,  $I_{BK}$  channels would be activated only during large depolarizations or when [Ca<sup>2+</sup>]<sub>i</sub> is increased.

$P_{open}$  at different voltages was measured in cell-attached patches with K<sup>+</sup> Ringer's solution in the bath to "clamp" the resting potential near 0 mV. The total number of  $I_{BK}$  channels present was estimated in several ways described in Materials and Methods. Figure 7 illustrates the voltage dependence of  $P_{open}$  in a patch estimated to contain 12  $I_{BK}$  channels. Superimposed on

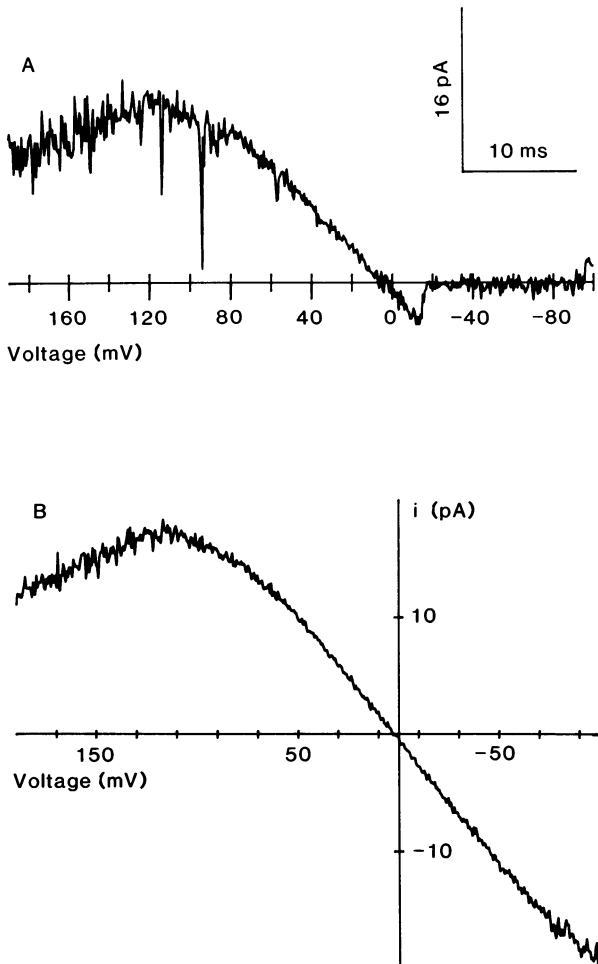


**Fig. 5.** (A) Single  $I_{BK}$  channel current in a cell-attached patch. One channel was open at the beginning of the ramp and except for brief closures, remained open to about  $-20$  mV. The bath contained  $K^+$  Ringer's solution to depolarize the resting potential of the cell; in ramps like this one in which a channel was open at  $V_{rev}$ , the current reversed consistently at  $+2$  mV, indicating that the membrane potential was kept near  $0$  mV. The voltage was ramped rapidly from positive to negative so that open channels would stay open to more negative potentials than during up ramps. The averaged current from ramps or segments of ramps in which no channels were open has been subtracted from the current record. The negative conductance region positive to  $+100$  mV was observed consistently, and was also observed when the voltage was ramped from negative to positive. (B) Single  $I_{BK}$  open-channel current-voltage relationship for the same experiment illustrated in A. The average of ramp current segments selected when no channels were open was subtracted from the average of currents selected when one channel was open. The slope conductance at its maximum (near  $V_{rev}$ ) was  $220$  pS.

the data points is the  $P_{open}$ - $V$  relationship fitted by a Boltzmann distribution, which was forced to limit at 0.95. The average  $V_{1/2}$  from similar fits in six patches was  $+171 \pm 18$  mV (mean  $\pm$  SD), with an average slope factor,  $V_{slope}$ ,  $-19.6 \pm 6.2$  mV. Because of errors in the estimate on  $N$  and the possibility that  $K^+$  Ringer's in the

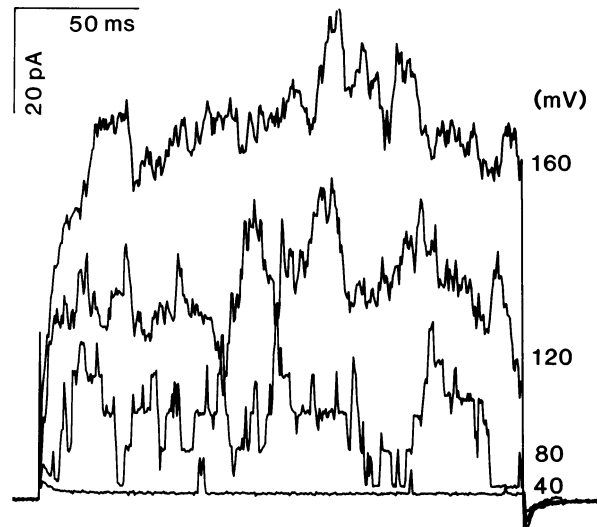


**Fig. 6.**  $I_{BK}$  currents in a cell-attached patch. From  $V_{hold} = 0$  mV pulses were applied, with currents illustrated at  $40$  mV increments. Discrete single-channel levels can be seen up to  $+80$  mV, but at more positive potentials they are not clearly distinguishable. Pipette contained  $KMeSO_3$  and the bath  $K^+$  Ringer's solution. Filter 1 kHz, sample interval 0.5 msec.

bath may not clamp the resting potential perfectly, especially in patches with large  $I_{BK}$  currents, these values should be considered quite approximate. Most estimates of the voltage dependence of  $I_{BK}$  channel opening range 10–15 mV/e-fold (Rudy, 1988).

The  $[Ca^{2+}]_i$  dependence of  $I_{BK}$  channels could be defined in excised inside-out patches. Figure 8 illustrates an experiment on an inside-out patch which contained 5  $I_{BK}$  channels and remained stable for about two hours. The left-hand panel illustrates superimposed patch currents during 8 consecutive pulses to each of several depolarizing voltages. The bath, corresponding to the intracellular solution, contained  $1 \mu M$   $[Ca^{2+}]$ . Several properties are apparent. First,  $P_{open}$  is voltage dependent. Only two openings were seen at  $+20$  mV. At  $+40$  mV, one channel was open often, and occasionally two. At  $+100$  mV, all six current levels are distinct, with all 5 channels open in some pulses. It is also evident that it takes some time for the channels to reach their steady-state  $P_{open}$  at a given potential. At each potential, most channels were initially closed, with  $P_{open}$  increasing during the pulses.

To determine the steady-state  $P_{open}$  at various voltages and  $[Ca^{2+}]_i$ , currents were recorded continuously at several  $V_{hold}$ . Amplitude histograms were constructed to determine the probability of each number,  $r$ , of open channels,  $P(r)$  (cf. Eq. 1), and finally  $P_{open}$  was calculated as:

$$P_{open} = \{\sum r P(r)\}/N \quad r = 1, 2, \dots, N \quad (2)$$

where  $N$  is the total number of channels, five in this patch. The open probability at three  $[Ca^{2+}]_i$  and several

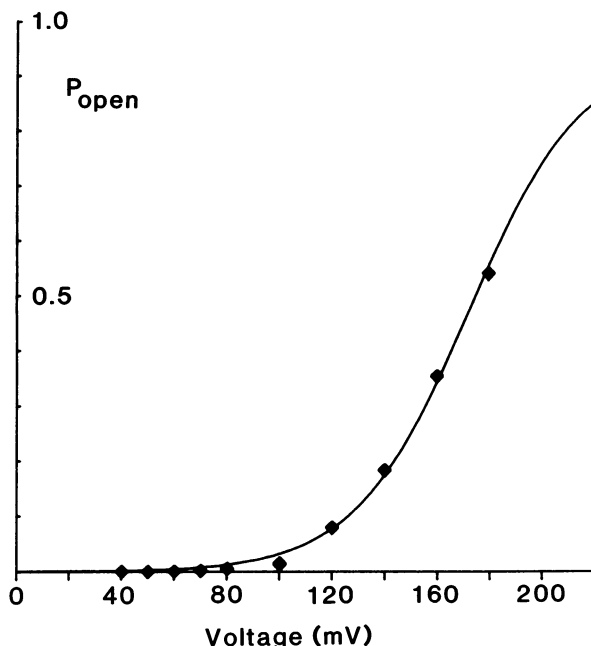


**Fig. 7.** Open probability,  $P_{\text{open}}$ , of  $I_{\text{BK}}$  channels in a cell-attached patch. The bath contained  $\text{K}^+$  Ringer's solution, and data are plotted assuming that the membrane potential was 0 mV. There were 12  $I_{\text{BK}}$  channels in this patch, determined from thirteen discrete levels of current seen at +180 mV, and reasonable agreement between the observed probability of observing each level and that calculated with the binomial theorem (see Materials and Methods). The curve shows the best-fitting (by nonlinear least squares) Boltzmann, with maximum  $P_{\text{open}}$  constrained at 0.95 because it was not well-defined by these data, with fitted  $V_{1/2} = 172$  mV and  $V_{\text{slope}} = -21.7$  mV.

voltages is plotted in Fig. 8B. At 3  $\mu\text{M}$   $[\text{Ca}^{2+}]_i$ ,  $P_{\text{open}}$  increased from nearly 0 at -60 mV to nearly 1.0 at +40 mV. Increasing  $[\text{Ca}^{2+}]_i$  to 10  $\mu\text{M}$  shifted  $P_{\text{open}}$  to more negative potentials, increasing  $P_{\text{open}}$  at each potential. The maximum  $P_{\text{open}}$  was 0.97–0.98, similar to previous observations in other cells. Lowering  $[\text{Ca}^{2+}]_i$  to 300 nM shifted the  $P_{\text{open}}\text{-}V$  relationship to more positive potentials. Comparison with  $P_{\text{open}}\text{-}V$  relationships in cell-attached patches (Fig. 7) suggests that  $[\text{Ca}^{2+}]_i < 300$  nM in intact THP-1 cells. The slope factor at 3  $\mu\text{M}$   $[\text{Ca}^{2+}]_i$  in Fig. 8 was -10 mV, comparable with that reported in other cells (Rudy, 1988), whereas in cell-attached patch configuration the apparent slope was less steep, with  $V_{\text{slope}}$  nearly -20 mV (cf. Fig. 7). Because of the possibility that the membrane potential of the cell changes due to the large  $I_{\text{BK}}$  currents flowing through the cell-attached patch membrane, especially at large positive potentials, the excised patch data are more reliable.

Macroscopic  $I_{\text{BK}}$  was seen in the whole-cell configuration, and resembled that described in human macrophages (Gallin & McKinney, 1988). Its identification was complicated in some cells by the presence of other channels, particularly chloride ( $I_{\text{Cl}}$ ) and nonselective cation ( $I_{\text{cat}}$ ). Nevertheless, in many cells  $I_{\text{BK}}$  was clearly

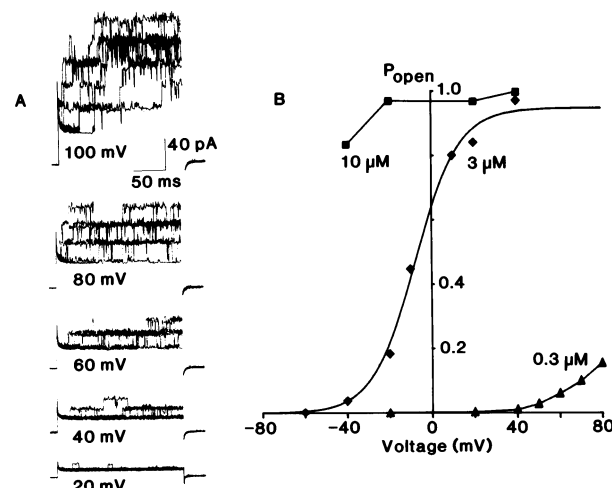


**Fig. 8.** (A) Voltage and time dependence of  $I_{\text{BK}}$  currents in an excised inside-out patch. Pipette 3  $\mu\text{M}$   $[\text{Ca}^{2+}]$  KMeSO<sub>3</sub> solution, bath 1  $\mu\text{M}$   $[\text{Ca}^{2+}]$  KMeSO<sub>3</sub> solution. Currents recorded during 8 consecutive pulses to each of the indicated potentials are superimposed. There were five  $I_{\text{BK}}$  channels in this patch, which was stable for more than an hour. Superimposed on these records is chatter due to a smaller channel which appeared to be voltage independent. (B) Steady-state open probability,  $P_{\text{open}}$ , for the  $I_{\text{BK}}$  channels in the patch illustrated in A. Measurements were made with bath (i.e., internal) solutions containing 0.3  $\mu\text{M}$  ( $\blacktriangle$ ), 3  $\mu\text{M}$  ( $\blacklozenge$ ), or 10  $\mu\text{M}$  ( $\blacksquare$ )  $[\text{Ca}^{2+}]$ . The curve shows the best-fitting simple Boltzmann function to the data at 3  $\mu\text{M}$   $[\text{Ca}^{2+}]$ , with midpoint,  $V_{1/2} = -7.5$  mV, slope factor,  $V_{\text{slope}} = -10.3$  mV, and  $P_{\text{open},\text{max}} = 0.946$ ; data at other  $[\text{Ca}^{2+}]$  are connected by lines for clarity. Currents were recorded continuously at each potential, amplitude histograms constructed, and the area under each peak calculated, to obtain  $P_{\text{open}}$ . See text and Eq. (2) for details. The largest number of channels ever observed to be open simultaneously in this patch was 5, setting  $N$ . The data were in excellent agreement with the predictions of binomial theorem for five identical, independent channels.

evident, characterized by its large fluctuations, its activation only during rather large depolarizations, its moderately rapid activation, and its lack of inactivation. Whole-cell currents with a clear  $I_{\text{BK}}$  component are illustrated in Fig. 9. A few single  $I_{\text{BK}}$  channel openings are evident at +40 mV and the current rapidly increased in amplitude with further depolarization. When the bath  $\text{Cl}^-$  was replaced by MeSO<sub>3</sub><sup>-</sup> (B), the noisy fluctuations attributed to  $I_{\text{BK}}$  were still present, but the pedestal of current at all positive potentials was reduced. Most of the time-independent current pedestal is thus attributable to anion current, which was reduced but not abolished in MeSO<sub>3</sub><sup>-</sup> solutions. Further depolarization elicited larger  $I_{\text{BK}}$  currents, as illustrated in Fig. 9C, in the same cell at lower gain. The  $I_{\text{BK}}$  currents in Fig. 9B and C are quite similar to those in the cell-attached patch illustrated in Fig. 6. Within about 100 msec after the start of each pulse,  $I_{\text{BK}}$  reached a steady-state level of activation and thereafter appeared to be time-independent, with no inactivation.

Block of  $I_{\text{BK}}$  by TEA<sup>+</sup> is illustrated in Fig. 10. Typi-

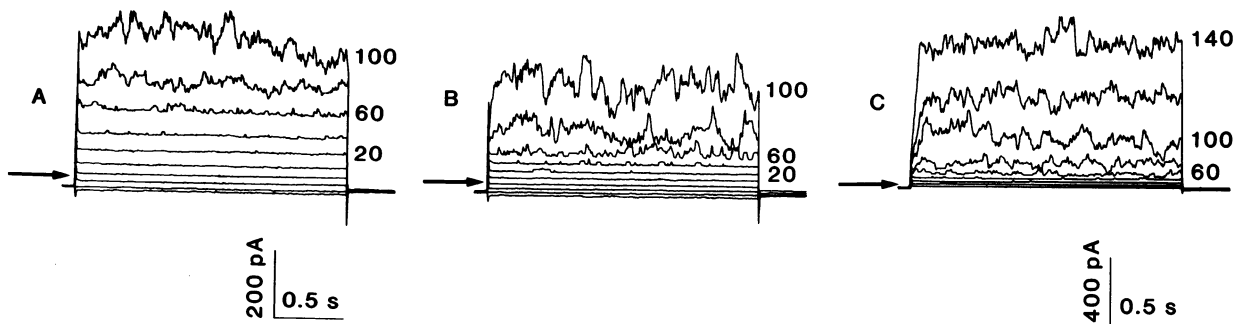


**Fig. 9.**  $I_{BK}$  currents in Ringer's solution with  $Cl^-$  (A) with  $Cl^-$  replaced by  $MeSO_3^-$  (B). In both solutions identical pulse families are plotted, in 20 mV increments between  $-80$  and  $+100$  mV, from  $V_{hold} = -60$  mV. (C) Same conditions as in B, but the gain is lower, and the voltage range extends from  $-20$  to  $+140$  mV. Arrows indicate zero current. The calibration bars on the left apply to both A and B. Filter 2 kHz in A and 1 kHz in B and C. Pipette contained KMeSO<sub>3</sub> solution, with nominally 38 nM  $Ca^{2+}$ .

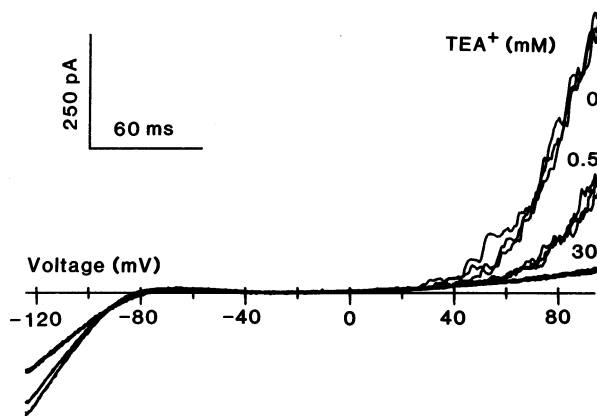


**Fig. 10.** Whole-cell ramp currents in a cell with prominent  $I_{IR}$  and  $I_{BK}$  currents. The bath contained Ringer's solution, the pipette KCl, with nominally 38 nM  $Ca^{2+}$ . Three consecutive ramps in each solution are superimposed. The traces are labeled according to the concentration of TEA<sup>+</sup> added, and the 0 TEA<sup>+</sup> data were recorded after washout of 30 mM TEA<sup>+</sup>. The  $I_{IR}$  current was rapidly and reversibly reduced by 30 mM TEA<sup>+</sup>. Although the  $I_{IR}$  current was slightly larger in 0.5 mM TEA<sup>+</sup> than in Ringer's, this may reflect incomplete washout of TEA<sup>+</sup>.

cal of PMA-differentiated cells, there was prominent  $I_{IR}$  current at potentials negative to  $E_K$ , and  $I_{BK}$  which is evident positive to about +20 mV.  $I_{BK}$  exhibits characteristically large fluctuations. Addition of 0.5 mM TEA<sup>+</sup> to the bath solution reduced the outward current by >50%. Thirty mM TEA<sup>+</sup> virtually abolished the outward current. In other experiments in which several concentrations of TEA<sup>+</sup> were applied, the half-blocking concentration of TEA<sup>+</sup> was estimated to be 0.35 mM for  $I_{BK}$ . TEA<sup>+</sup> inhibited  $I_{IR}$  weakly; 30 mM TEA<sup>+</sup> rapidly and reversibly reduced  $I_{IR}$  by about 30%.

#### CHANGES IN ION CHANNEL EXPRESSION DURING DIFFERENTIATION OF THP-1 CELLS

The Table summarizes the occurrence and amplitudes of the major ion channels found in THP-1 cells before and

after differentiation by PMA. Undifferentiated THP-1 monocytes consistently expressed five channels:  $I_{DR}$ ,  $I_{SK}$ ,  $I_H$ ,  $I_{cat}$ , and  $I_{Cl}$ . PMA-differentiated cells expressed six ion channels:  $I_{IR}$ ,  $I_{BK}$ ,  $I_{SK}$ ,  $I_H$ ,  $I_{cat}$ , and  $I_{Cl}$ .  $I_{IR}$  and  $I_{BK}$  were found almost exclusively in differentiated cells,  $I_{DR}$  was found almost exclusively in undifferentiated cells, while  $I_{SK}$ ,  $I_{Cl}$ ,  $I_H$ , and  $I_{cat}$  were found in both. In the following, we describe the criteria used to decide whether a particular channel was present.

#### Delayed Rectifier, $I_{DR}$

Nearly all undifferentiated THP-1 cells tested in Ringer's solution (99%, Table) expressed  $I_{DR}$ . The presence of  $I_{DR}$  was established by its characteristic inactivation with  $\tau_i$  several hundred msec and slow recovery.  $I_{DR}$  was activated by depolarization above threshold potentials and decreased progressively during repeated voltage ramps (illustrated in Fig. 2B, Kim et al., 1996). The amplitudes summarized in the Table are the difference between the currents at +80 mV during the first and last ramp, i.e., the inactivating component of outward current, and therefore underestimate  $I_{DR}$ , but unequivocally reflect this conductance. No other channels in these cells inactivated. The average amplitude of  $I_{DR}$  was 378 pA at +80 mV in control THP-1 cells. This conductance was rarely (4%) detected in differentiated cells.

#### $Ca^{2+}$ -activated $K^+$ Channels, $I_{SK}$

When 10  $\mu$ M  $Ca^{2+}$  was present in the internal solution, a time-independent  $K^+$  conductance,  $I_{SK}$ , was present in every cell studied. Even using the "standard" pipette solution, with  $[Ca^{2+}]_i$  buffered to nominally 38 nM, there were small currents resembling  $I_{SK}$  in some cells. This may mean that this conductance is activated to a small extent even at low  $[Ca^{2+}]_i$ , but could also reflect imperfect control of  $[Ca^{2+}]_i$  by EGTA, which is a rather slow  $Ca^{2+}$  buffer. Because it is not voltage-gated,  $I_{SK}$  is difficult to isolate from other conductances. We therefore

**Table.** Ion channel expression during THP-1 cell differentiation

Channel	Undifferentiated monocytes		PMA-differentiated macrophages	
	% expressing	Amplitude	% expressing	Amplitude
$I_{DR}$ (pA)	99 (81/82)	378 $\pm$ 339 (57)	4 (2/45)	60
$I_{SK}$ (nS)	100 (22/22)	2.3 $\pm$ 1.8 (21)	100 (5/5)	
$I_{BK}$ (no. in patch)	0 (0/24)		38 (11/29)	14 $\pm$ 16 (9)
$I_{IR}$ (nS)	1 (1/82)	1.8	70 (31/44)	5.6 $\pm$ 5.5 (28)
$I_H$ (pA/pF)	present	16.6 $\pm$ 8.8 (10)	present	7.2 $\pm$ 5.2 (22)
$I_{cat}$ (nS)	66 (37/56)		present	32 $\pm$ 33 (6)
$I_{Cl}$	89 (8/9)		100 (12/12)	

In each case, expression is the percent of cells studied under appropriate conditions judged to express the conductance (expressing/total). Amplitudes are mean  $\pm$  SD for ( $n$ ) cells, including only cells expressing the conductance.  $I_{DR}$  amplitude is the current at +80 mV which inactivated during repeated voltage ramps in Ringer's solution with K<sup>+</sup>-containing pipette solutions with < 3  $\mu$ M Ca<sup>2+</sup>.  $I_{SK}$  amplitude is the slope conductance measured at  $V_{rev}$  in Ringer's solution in cells studied at 10  $\mu$ M [Ca<sup>2+</sup>].  $I_{BK}$  amplitude is the estimated number of channels per cell-attached patch.  $I_{IR}$  amplitude is the slope conductance in Ringer's solution near -100 mV, after subtraction of leak estimated at more positive potentials.  $I_H$  was seen in nearly every cell.  $I_H$  at +40 mV at pH<sub>o</sub> 7.0//pH<sub>i</sub> 5.5 is normalized to cell size and was taken from Fig. 2, DeCoursey & Cherny, 1996.  $I_{cat}$  is the slope conductance between +80 and +100 mV for pipette solutions with K<sup>+</sup> or Na<sup>+</sup> as the cation; in 9 cells studied with TMA<sup>+</sup> in the pipette  $I_{cat}$  was not seen.  $I_{Cl}$  was studied with TMACl or TEAMeSO<sub>3</sub> pipette solutions to preclude other outward current carriers, and was considered present if outward current was reduced when Cl<sup>-</sup> was replaced with MeSO<sub>3</sub><sup>-</sup>. See text for further details.

arbitrarily quantitated  $I_{SK}$  only when the whole-cell currents reversed negative to -60 mV in Ringer's solution. Because the  $I_{SK}$  amplitude was not well-determined, we have not attempted to compare its amplitude in control and differentiated THP-1 cells. The value for the slope conductance of  $I_{SK}$  is given in the Table only as a general benchmark.

#### $Ca^{2+}$ -activated "maxi" K<sup>+</sup> Channels, $I_{BK}$

The entries in the Table for  $I_{BK}$  include only observations in cell-attached patches. We saw  $I_{BK}$  in many whole-cell experiments (e.g., Figs. 9 and 10) (only in differentiated THP-1 cells), but could not reliably estimate its amplitude due to the possibility that other conductances ( $I_{Cl}$ ,  $I_{cat}$ ) might be present. Maxi-K<sup>+</sup> channels were searched for in cell-attached patches by ramping the voltage rapidly from RP + 190 mV down to RP - 40 mV, after a ~55 msec prepulse to RP + 190 mV. When  $I_{BK}$  channels were present, they usually were elicited by this procedure. If no channels were observed in ~200 ramps, the  $I_{BK}$  channel was considered absent in that patch. Numbers of channels were estimated as described in Materials and Methods.  $I_{BK}$  channels were often observed in patches or in whole-cell records of differentiated THP-1 cells, but were never observed in control THP-1 cells.

#### Inwardly-rectifying K<sup>+</sup> Channels, $I_{IR}$

$I_{IR}$  was defined by a clear inflection of inward current negative to  $E_K$ . In contrast,  $I_{SK}$  does not exhibit this

inflection, but has a more uniform conductance in this voltage range. In many, but not all cells, the bath was changed from Ringer's solution to K<sup>+</sup> Ringer's to confirm the shift with  $E_K$  of the voltage range of activation of  $I_{IR}$ , and to increase the  $I_{IR}$  amplitude.  $I_{IR}$  was almost never seen in undifferentiated THP-1 monocytes, but was present in the majority of differentiated THP-1 macrophages.

#### $H^+$ Currents, $I_H$

Voltage-activated H<sup>+</sup> selective currents were observed both in undifferentiated and differentiated THP-1 cells. The properties of these currents, and changes during differentiation are described elsewhere (DeCoursey & Cherny, 1996). H<sup>+</sup> current activation was slower and its density decreased by about one-half in differentiated cells.

#### Nonselective Cation Currents, $I_{cat}$

A time-independent outward current ( $I_{cat}$ ) was observed in addition to the inactivating outward K<sup>+</sup> current in two-thirds of undifferentiated THP-1 monocytes. This conductance was observed with K<sup>+</sup> (32/49) or Na<sup>+</sup> (5/7) but not TMA<sup>+</sup> (0/9) in the pipette solution. Therefore this channel conducts small cations rather indiscriminately, but not large cations. The data in the Table therefore

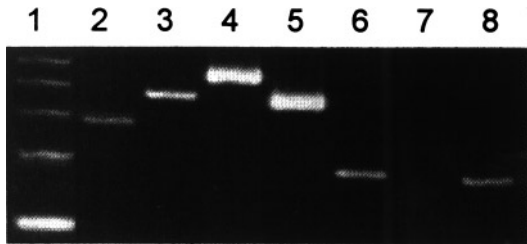


**Fig. 11.** Identification of channels expressed in THP-1 cells. DNA was amplified by PCR and stained with ethidium bromide after electrophoresis in an agarose gel. Lane 1, molecular weight marker increasing in 123 BP increments (from bottom to top). Lane 2, reverse transcription was applied to isolated RNA from PMA-differentiated THP-1 cells, followed by PCR to amplify cDNA using IRK1 primers. Lane 3, same procedure as lane 2 using primers for Kv1.3 on cDNA from undifferentiated THP-1 cells. Lane 4, competitor DNA used for measurement of Kv1.3 cDNA. Lane 5, competitor DNA for measurement of IRK1 cDNA. Lane 6, DNA amplified by PCR applied to human genomic DNA using the G3PDH primer set. Lane 7, PCR using G3PDH primers was applied to a RNA sample in which reverse transcription was absent. Lane 8, same procedure as lane 2 and amplified with G3PDH primers. Comparison of lanes 7 and 8 reveals reverse transcription is required for amplification of DNA from total RNA, confirming that the bands originate from mRNA. Note that amplification of IRK1 and Kv1.3 cDNA in samples from THP-1 cells indicates that mRNA for these two types of channels is represented.

include only  $K^+$  and  $Na^+$  pipette solutions.  $I_{cat}$  increased dramatically with depolarization during either voltage ramps or pulses. In ramps  $I_{cat}$  did not inactivate, in contrast with  $I_{DR}$ ; in pulses it was time independent.  $I_{cat}$  was not reduced when  $Cl^-$  in the bath was replaced with  $MeSO_3^-$ . Given the development of  $I_{cat}$  with time in whole-cell configuration and the possible presence of other currents, the amplitude of  $I_{cat}$  should be considered approximate.  $I_{cat}$  was clearly present in some differentiated THP-1 macrophages, but in cells with large  $I_{BK}$  currents, the presence of  $I_{cat}$  was hard to establish. Therefore we cannot determine whether its expression changed after differentiation.

#### Chloride Current $I_{Cl}$

$I_{Cl}$  was considered present when replacing  $Cl^-$  with  $MeSO_3^-$  reduced the outward current and shifted  $V_{rev}$  to more positive potentials.  $I_{Cl}$  was present in practically all THP-1 cells in which it was searched for, regardless of state of differentiation.  $I_{Cl}$  ran down fairly rapidly in THP-1 cells, and was not studied extensively. Its transience precludes meaningful quantitative comparisons.

#### MOLECULAR IDENTIFICATION OF CHANNELS EXPRESSED IN THP-1 CELLS

The physiological and pharmacological characteristics of the whole cell currents were consistent with a prediction

that Kv1.3 was responsible for  $I_{DR}$  and IRK1 for  $I_{IR}$ . We therefore tested, by PCR of cDNA, whether mRNA associated with these channel types was present in THP-1 cells. Total RNA was reverse-transcribed, and the cDNA was amplified by PCR employing primers with sequences specific for one of the two types of channel. A gel showing the amplified products is shown in Fig. 11. The DNA band obtained following PCR with the Kv1.3 primer set (lane 3) was the size predicted from the known sequence, 478 BP (K. Folander, S. Lin, G. Koo, and R. Swanson, *unpublished*, GenBank locus HUMPOCH). The band obtained using the IRK1 primer set (lane 2) was also of the predicted size based on the sequence of human heart IRK1, 356 BP (Raab-Graham, Radeke & Vandenberg, 1994). The gel also shows bands of DNA in two lanes which were constructed to be used for the competitive PCR assay of mRNA levels (see below).

Because amplified DNA could possibly originate from genomic, rather than cDNA, we tested for the presence of genomic DNA in the total RNA samples. A typical example experiment is also shown on the gel in Fig. 11. G3PDH can routinely be amplified from human genomic DNA (lane 6). Although G3PDH cDNA could be amplified from total RNA following reverse transcription (lane 8), no amplification was obtained for PCR of total RNA from the same isolation but without reverse transcription (lane 7). This result indicates that genomic DNA is not present in the sample. Although the G3PDH gene has a small intron in the amplified region (Ercolani et al., 1988), the genome contains numerous processed pseudogenes (Arcari, Martinelli & Salvatore, 1989) which likely are amplified in this procedure.

#### Comparison of Sequence with Known Channels

We used a BLAST analysis (Altschul et al., 1990) to compare the sequence of our cDNA fragments with all known sequences in the GenBank and EMBL databases (657,579 sequences). To positively identify the PCR products obtained using the channel primers, we partially sequenced the resulting cDNA. The sequence obtained in single-pass sequencing for the IRK1 cDNA fragment of 195 bases in fact matched that of nucleotides 949 to 1145 of the known sequence for the human inward rectifier channel HH-IRK1 (Raab-Graham et al., 1994). A partial (260 base) sequence from our Kv1.3 product exactly matched that of nucleotides 1109 to 1369 for the human voltage-gated  $K^+$  channel Kv1.3 (Folander et al., *loc cit*; *see also* Cai et al., 1992). The results therefore indicate that both IRK1 and Kv1.3  $K^+$  channel mRNA species are found in THP-1 cells, suggesting that these channels contribute to the inward and outward membrane currents respectively.

## CHANGES IN mRNA ABUNDANCE IN THP-1 CELLS AFTER DIFFERENTIATION

As described above and in the Table,  $I_{DR}$  was present in almost all undifferentiated THP-1 monocytes but almost never in differentiated macrophages, whereas  $I_{IR}$  was found almost exclusively in differentiated cells. We explored whether changes in mRNA abundance could explain these changes in  $K^+$  channel expression. The levels of mRNA associated with the IRK1 and Kv1.3 channels were measured in differentiated cells and in a matched culture of undifferentiated cells. The results of a competitive PCR experiment which determined changes in mRNA following differentiation are shown in Fig. 12A. In this experiment, cDNA following reverse transcription of total RNA was amplified in the presence of a competitor DNA. As the amount of competitor added was increased, the ratio of competitor to channel cDNA which was amplified decreased. Note in the figure that for IRK1 at any concentration of competitor the ratio of channel to competitor DNA amplified is greater for the sample from the differentiated cells, indicating that there was more cDNA present. Because the cDNA in each sample is derived from a constant amount of total RNA, the difference in cDNA is associated with a difference in mRNA for this species of channel. A difference in Kv1.3 mRNA was also found, as shown in Fig. 12B. In these same RNA samples, the amount of Kv1.3 mRNA was less in the differentiated cells.

The change in the concentration of competitor giving equal amplification of channel cDNA and competitor DNA ( $\log \text{ratio} = 0$ ) was used to determine the percent difference in cDNA between two samples. The abundance of mRNA for IRK1 in undifferentiated monocytes was only 20% of the level found in matched cultures of differentiated cells in two experiments and was only 1% in a third experiment. In the same samples, the level of Kv1.3 mRNA in differentiated THP-1 macrophages decreased to  $13.7 \pm 8.6\%$  (mean  $\pm$  SE,  $n = 3$ ) of the value found in undifferentiated cells. Thus, although there was substantial variability, there was a dramatic decrease in mRNA for Kv1.3 and a large increase in mRNA for IRK1 in differentiated cells.

## Discussion

### INWARDLY RECTIFYING $K^+$ CURRENT, $I_{IR}$

#### Properties

$I_{IR}$  channels in PMA-differentiated THP-1 macrophages exhibit all of the properties of classical “strong” inward rectifiers. There are large inward currents negative to  $E_K$  and a small bump of outward current which decreases to

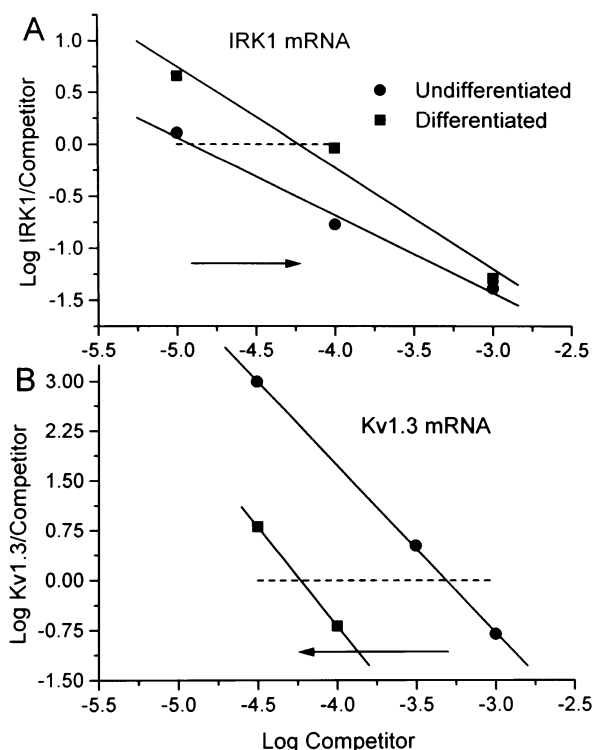


**Fig. 12.** Determination of changes in IRK1 and Kv1.3 mRNA inferred using competitive PCR of cDNA. (A) PCR was applied simultaneously to cDNA obtained from either undifferentiated or differentiated THP-1 cells. The ratio of the signal associated with amplified IRK1, relative to that of the competitor, was measured as the concentration of competitor was increased. The concentration of competitor added to obtain a ratio of 1 ( $\log 1 = 0$ ) was higher in the sample from differentiated cells, indicating that the cDNA in that sample was greater. The direction and magnitude of the increase is shown by the arrow. The concentration of the competitor is given as the dilution of a stock of 100 attomoles/ $\mu\text{l}$ . (B) Kv1.3 cDNA was measured from the same cDNA samples used for the experiment shown in A. Note that the level of Kv1.3 cDNA is higher in the sample from undifferentiated cells.

zero within about 50 mV positive to  $E_K$ . The single channel conductance in symmetrical high  $[K^+]$  is about 30 pS, and in cell-attached patches no outward  $I_{IR}$  current can be detected. The  $I_{IR}$  turns on with time during hyperpolarizing pulses in a  $[K^+]_o$ - and voltage-dependent manner. This time-dependent turn-on has been interpreted as an “intrinsic gating” process in other cells (e.g., Matsuda, Saigusa & Irisawa, 1987; Silver & DeCoursey, 1990), and recently has been ascribed to a voltage-dependent unblock by intracellular polyamines (Fakler et al., 1994; Lopatin, Makhina & Nichols, 1994). In any case, this time-dependence is another hallmark of  $I_{IR}$  currents. The voltage-activation relationship shifts along the voltage axis in parallel with  $V_{rev}$  when  $[K^+]_o$  is varied.  $I_{IR}$  is blocked in a voltage-dependent manner, with block increasing with hyperpolarization, by  $\text{Na}^+$ ,  $\text{Cs}^+$ ,

and  $\text{Ba}^{2+}$ . Block by  $\text{Na}^+$  and  $\text{Ba}^{2+}$  is time-dependent, with the rate of block increasing with hyperpolarization; any time-dependence of  $\text{Cs}^+$  block was too fast to resolve.

### Expression in Other Monocytes

$I_{\text{IR}}$  in THP-1 cells is similar to that in mouse peritoneal macrophages (Gallin & Livengood, 1981), J774 cells (Gallin & Sheehy, 1985; Gallin & McKinney, 1988; McKinney & Gallin, 1988), HL-60 cells differentiated into macrophage-like cells (Wieland, Chou & Gong, 1990), rabbit osteoclasts (Kelly, Dixon & Sims, 1992), and microglia (Kettenmann, Banati & Walz, 1993).  $I_{\text{IR}}$  expression changes predictably in several macrophage-related cells.  $I_{\text{IR}}$  appears in J774.1 cells 2–4 hr after plating, and is expressed in all cells after adherence (Gallin & Sheehy, 1985); the increase in  $I_{\text{IR}}$  channel density was prevented by cyclohexamide (McKinney & Gallin, 1990).  $I_{\text{IR}}$  appears in murine macrophages after a few days in culture (Gallin & Livengood, 1981; Randriamampita & Trautmann, 1987). HL-60 cells develop  $I_{\text{IR}}$  when induced by PMA to differentiate into macrophages, but not when induced to differentiate along the granulocyte lineage (Wieland et al., 1990). Rat osteoclasts with spread morphology expressed  $I_{\text{IR}}$ , whereas those with rounded shape expressed  $I_{\text{DR}}$  (Arkett, Dixon & Sims, 1992). In human monocyte-derived macrophages, however, expression of  $I_{\text{IR}}$  was independent of adherence or time in culture (Nelson, Jow & Jow, 1990a). We observed  $I_{\text{IR}}$  rarely in undifferentiated THP-1 monocytes, but in a majority of PMA-differentiated (and adherent) macrophages (Table). The general pattern emerging from most studies is that  $I_{\text{IR}}$  expression in macrophages appears to be correlated with adherence or with differentiation. Because there are quite real differences between macrophages in different tissues and at different stages of differentiation and activation, more explicit generalization may not be possible or fruitful.

### Possible Functions of $I_{\text{IR}}$

There is substantial evidence that  $I_{\text{IR}}$  helps maintain a large negative resting potential in macrophages (Gallin & Livengood, 1981; Gallin & Sheehy, 1985; McKinney & Gallin, 1990; see Gallin, 1991). In undifferentiated THP-1 cells lacking  $I_{\text{IR}}$ ,  $I_{\text{DR}}$  may be capable of setting the resting potential, although its threshold would likely keep the resting potential at somewhat more positive values (e.g., -50 to -60 mV) than would  $I_{\text{IR}}$ . The appearance of  $I_{\text{IR}}$  in differentiated THP-1 cells may reflect a need for the cell to have a more negative resting potential. The reciprocal expression of  $I_{\text{IR}}$  and  $I_{\text{DR}}$ , however, provides THP-1 cells with a  $\text{K}^+$  channel capable of

setting the resting potential at all stages of differentiation.

### LARGE CONDUCTANCE $\text{Ca}^{2+}$ -ACTIVATED “MAXI K” CHANNEL, $I_{\text{BK}}$

#### Properties

$I_{\text{BK}}$  in differentiated THP-1 cells is quite similar to  $I_{\text{BK}}$  channels described in a wide variety of cells.  $I_{\text{BK}}$  channels are activated by a combination of intracellular  $\text{Ca}^{2+}$  and membrane depolarization. At physiological  $[\text{Ca}^{2+}]_i$   $I_{\text{BK}}$  was active only at large positive membrane potentials, e.g., >+40 mV, as can be seen either from the  $[\text{Ca}^{2+}]_i$  dependence in inside-out patches, or in cell-attached patches, in which channels were exposed to cytoplasmic  $[\text{Ca}^{2+}]_i$ . Increasing  $[\text{Ca}^{2+}]_i$  shifts the voltage-activation relationship to more negative potentials; thus,  $I_{\text{BK}}$  can be activated by increases in  $[\text{Ca}^{2+}]_i$ , especially when coupled with membrane depolarization.  $I_{\text{BK}}$  channels have a large unitary conductance, 200–250 pS at symmetrical high  $[\text{K}^+]$ . In cell-attached patches single-channel currents exhibited pronounced negative slope conductance at large positive potentials (>+80 mV), consistent with rapid voltage-dependent block by cytoplasmic  $\text{Na}^+$  (Marty, 1983). Macroscopic  $I_{\text{BK}}$  is noisy because of the large unitary conductance, and is potently blocked by external  $\text{TEA}^+$ , with half-block at <0.5 mM, consistent with  $I_{\text{BK}}$  behavior in other cells (Rudy, 1988).

### Expression in Other Monocytes

$I_{\text{BK}}$  in human macrophages has been described in both single-channel (Gallin, 1984) and whole-cell studies (Gallin & McKinney, 1988). A similar channel is present in chick osteoblasts (Ravesloot et al., 1990) and rabbit osteoclasts (Weidema et al., 1993). In the latter study, the characteristic negative slope conductance prominently observed in  $I_{\text{BK}}$  channels in cell-attached patches was shown to be due to voltage-dependent block by intracellular  $\text{Na}^+$ , as first shown in chromaffin cells by Marty (1983).

$I_{\text{BK}}$  is absent from most human peripheral blood macrophages, but expression increases to >90% after 1–2 weeks in culture (Gallin & McKinney, 1988). Similarly,  $I_{\text{BK}}$  was absent from undifferentiated THP-1 monocytes, but was often present in PMA-differentiated macrophages (Table). An intriguing juxtaposition of  $I_{\text{IR}}$  and  $I_{\text{BK}}$  channels is seen in both differentiated THP-1 cells and cultured human macrophages (Gallin & McKinney, 1988).

### DELAYED RECTIFIER, $I_{\text{DR}}$

#### Expression in Other Monocytes

The predominance of  $I_{\text{DR}}$  in undifferentiated THP-1 monocytes contrasts sharply with its absence in most

PMA-differentiated THP-1 macrophages (Table). Other investigators have reported up- or down-regulation of  $I_{DR}$  in macrophages and related cells. Mouse peritoneal macrophages express  $I_{DR}$  after one to four days in culture (Ypey & Clapham, 1984), which then decreases after 5–6 days in culture (Randriamampita & Trautmann, 1987).  $I_{DR}$  was expressed in freshly-plated J774.1 cells but then disappeared, as  $I_{IR}$  became predominant (Gallin & Sheehy, 1985).  $I_{DR}$  expression in monocyte-derived macrophages increased after incubation with bacterial endotoxin, lipopolysaccharide (LPS), or with IL-2 (Nelson, Jow & Jow, 1992). Undifferentiated microglia, which are derived from monocytes, express  $I_{IR}$  (Kettenmann et al., 1990), but after induction by LPS to differentiate express  $I_{DR}$  as well (Nörenberg, Gebicke-Haerter & Illes, 1992).  $I_{DR}$  channels are expressed in the human myeloblastic leukemia cell line ML-1, but disappear after the cells are induced by PMA to differentiate terminally (Lu et al., 1993). In general, the  $I_{DR}$  conductance appears to develop a short time after cell isolation or cell adherence and often disappears over long-term culture.

In a number of cell types there appears to be a requirement for functional  $I_{DR}$  channels during proliferation.  $K^+$  channel blockers inhibit proliferation of human T lymphocytes (DeCoursey et al., 1984; Price, Lee & Deutsch, 1989). Unstimulated murine T lymphocytes express only a few  $I_{DR}$  channels per cell, but the channel density increases more than an order of magnitude 1–2 days after stimulation with mitogens (DeCoursey et al., 1987). Block of  $I_{DR}$  but not of  $Ca^{2+}$ -activated  $K^+$  currents inhibits growth and differentiation of brown fat cells (Pappone & Ortiz-Miranda, 1993).  $K^+$  channel blockers also inhibit proliferation of glia (Chiu & Wilson, 1989), neuroblastoma (Rouzaire-Dubois & Dubois, 1991), melanocytes (Nilius & Wohlrbab, 1992), and renal tubule cells (Teulon et al., 1992). Undifferentiated THP-1 cells which are actively proliferating express  $I_{DR}$ , but after differentiation  $I_{DR}$  disappears. Most of these results suggest a role for  $I_{DR}$  channels in actively proliferating cells.

#### Can $I_{DR}$ Channels Help Set the Resting Potential?

Two hypotheses proposed for the involvement of Kv1.3 channels in lymphocyte proliferation invoke roles in setting the membrane potential or in volume regulation. The resting potential of T lymphocytes averages  $-59$  mV (range  $-35$  to  $-72$  mV), is near the threshold for activating Kv1.3 channels, and fluctuates over a 20 mV range (Verheugen et al., 1995). Because the input resistance of these small cells is so high, only a few channels need open to significantly alter the membrane potential (Cahalan et al., 1985). ChTX and other toxin blockers of  $I_{DR}$  depolarize the membrane potential of T lymphocytes (Leonard et al., 1992). ChTX-sensitive, voltage-gated

$K^+$  channels also maintain the resting potential of human platelets (Mahaut-Smith et al., 1990). By maintaining a large negative membrane potential, Kv1.3 channels may facilitate influx via receptor-activated  $Ca^{2+}$  channels (Lewis & Cahalan, 1989; Leonard et al., 1992). Whether  $I_{DR}$  channels also contribute to maintaining the resting membrane potential of THP-1 cells would presumably depend on whether other  $K^+$  channels are present which might be active under physiological conditions.  $I_{IR}$ , if present, would be expected to predominate. If activated sufficiently,  $I_{SK}$  might set the membrane potential. But if  $I_{DR}$  is the only  $K^+$  channel active in a cell, it would prevent the membrane potential from depolarizing far beyond its threshold potential.

#### Do $I_{DR}$ Channels Participate in Volume Regulation?

The second hypothesis is based on the suggestion that Kv1.3 channels are activated during volume regulation in lymphocytes (DeCoursey et al., 1985; Cahalan & Lewis, 1988; Deutsch & Lee, 1988). This mechanism has been extended to include a role in lymphocyte proliferation (Deutsch & Lee, 1988; Rouzaire-Dubois & Dubois, 1991; Dubois & Rouzaire-Dubois, 1993). The sensitivity of both proliferation and volume regulation to Kv1.3 blockers is intriguing in light of the fact that block of Kv3.1, another depolarization-activated  $K^+$  channel in lymphocytes, inhibits neither mitogen-stimulated proliferation (DeCoursey et al., 1987) nor volume regulation (Deutsch & Chen, 1993). In contrast, neither ChTX nor 4-aminopyridine inhibited regulatory volume decrease in THP-1 cells (Gallin, Mason & Moran, 1994), thus  $I_{DR}$  apparently does not serve this function in THP-1 cells (see next section).

#### SMALL CONDUCTANCE $Ca^{2+}$ -ACTIVATED $K^+$ CHANNEL, $I_{SK}$

$I_{SK}$  was observed both in control and differentiated THP-1 cells. Macroscopic  $I_{SK}$  currents were reported in J774 and murine peritoneal macrophages (Randriamampita & Trautmann, 1987). An apparently similar macroscopic  $I_{SK}$  current is present in HL-60 promyelocytes, and also after differentiation by PMA into macrophages, but is suppressed in HL-60 cells differentiated into granulocytes by retinoic acid (Wieland et al., 1992).  $I_{SK}$  channels have been described in human macrophages, and in contrast with  $I_{BK}$  were present at all times in culture (Gallin, 1989). Most likely,  $I_{SK}$  is responsible for spontaneous membrane hyperpolarizations described in macrophages (Gallin et al., 1975). In general,  $I_{SK}$  appears to be expressed in macrophages more consistently than are several other  $K^+$  channels.

Because the opening of  $I_{SK}$  channels depends on

$[Ca^{2+}]_i$  and not on membrane potential, this conductance will be activated whenever  $[Ca^{2+}]_i$  is increased sufficiently. Our data indicate massive activation at >300 nM  $[Ca^{2+}]_i$ , and detectable  $I_{SK}$  current in a minority of cells even with a low  $[Ca^{2+}]$  pipette solution (nominally 46 nM). We interpret this latter result to poor control of  $[Ca^{2+}]_i$  in these cells, however, and expect that  $I_{SK}$  is at most minimally active at resting  $[Ca^{2+}]_i$ . The  $[Ca^{2+}]_i$  dependence observed here is in agreement with more quantitative studies in which both  $[Ca^{2+}]_i$  and  $I_{SK}$  were monitored simultaneously in individual lymphocytes (Grissmer, Nguyen & Cahalan, 1993; Verheugen et al., 1995). Any increase of  $[Ca^{2+}]_i$  above resting values will tend to activate  $I_{SK}$ .  $[Ca^{2+}]_i$  is increased in macrophages upon stimulation with a formyl peptide stimulating superoxide release (Stickle, Daniele & Holian, 1984), extracellular ATP (Sung et al., 1985), platelet activating factor, PAF (Conrad & Rink, 1986), or monocyte chemotactic protein-1, MCP-1 (Sozzani et al., 1993), and during Fc-receptor-mediated phagocytosis (Young, Ko & Cohn, 1984; Di Virgilio et al., 1988). However, an increase in  $[Ca^{2+}]_i$  is not regulatory for superoxide release (Stickle et al., 1984) or for phagocytosis (Di Virgilio et al., 1988). Those stimuli resulting in increases in  $[Ca^{2+}]_i$  would likely activate  $I_{SK}$ , resulting in  $K^+$  efflux and membrane hyperpolarization. This mechanism has been demonstrated in mitogen-stimulated rat thymocytes (Mahaut-Smith & Mason, 1991). In macrophages, ATP activates  $I_{SK}$  (Hara et al., 1990), presumably the result of  $Ca^{2+}$  influx through the ATP-induced conductance (Buisman et al., 1988).

Challenging THP-1 cells with hypotonic solutions increases  $[Ca^{2+}]_i$  and triggers regulatory volume decrease, mediated by both cation and anion conductances (Gallin et al., 1994). The pharmacology is somewhat suggestive of  $I_{SK}$  or possibly  $I_{IR}$  involvement in the cation fluxes, but existing data do not clearly identify the channel(s) responsible.

#### PCR STUDIES OF mRNA FOR $K^+$ CHANNELS

We provide evidence by PCR that the  $I_{IR}$  currents in human THP-1 cells are due to an IRK1-related channel like that cloned originally in the J774 macrophage cell line (Kubo et al., 1993). The evidence also suggests that the channel responsible for  $I_{DR}$  is Kv1.3, which has been found in human and rat lymphocytes (Douglass et al., 1990; Grissmer et al., 1990; Cai et al., 1992) and in rat microglia (Nörenberg et al., 1993).

Because the expression of these two  $K^+$  channels changed dramatically during differentiation, we tested whether these changes were reflected in mRNA abundance. The levels of mRNA for Kv1.3 decreased on average by 7-fold, whereas the mRNA for IRK1 increased on average 7-fold. The abundance of mRNA thus

roughly paralleled channel expression in undifferentiated and differentiated THP-1 cells, suggesting that changes in either the rate of transcription or of degradation of mRNA (or both) were responsible for a substantial part of the changes in channel expression. A more quantitative estimate of the change in the average number of channels per cell can be made by weighting the current amplitude (Table) by the percent of cells expressing that channel. By this calculation, expression of functional  $I_{DR}$  channels decreased 141-fold, and  $I_{IR}$  channel expression increased 180 times during differentiation. Based on these estimates of channel density, the numbers of functional channels changed by a factor at least an order-of-magnitude greater than did mRNA levels.

Comparisons between changes in  $K^+$  channel expression and corresponding mRNA levels in immune cells have been few. Cai et al. (1992) reported a marked decrease in Kv1.3 mRNA levels after stimulation with the mitogen concanavalin A, in contrast with the two-fold increase in  $I_{DR}$  observed in activated human T lymphocytes (Deutsch, Krause & Lee, 1989). However, the changes in  $K^+$  channel expression in activated human T lymphocytes were small, whereas the changes in THP-1 cells were dramatic. Nörenberg et al. (1993) failed to detect differences in mRNA levels for Kv1.3 in microglia after LPS treatment which increased the fraction of cells expressing  $I_{DR}$  from 7% to 92%, but concluded that this 13-fold increase in the number of cells expressing  $I_{DR}$  might not result in changes in mRNA detectable by their technique. We saw essentially no  $I_{IR}$  in control THP-1 cells, and almost never saw  $I_{DR}$  in differentiated THP-1 cells, with >100-fold changes in total channel expression. The changes in  $K^+$  channel mRNA levels in THP-1 cells were much smaller than those in channel expression, but the changes were still large and in the same direction. Thus, posttranscriptional events may play a role in modulating  $K^+$  channel expression. However, expression of functional channels at three days may reflect changes in mRNA levels occurring earlier and possibly subsiding. Thus, it is not surprising that mRNA levels measured at a specific time point may not correlate precisely with channel expression. Nevertheless, the observed general correlation between mRNA levels and  $K^+$  channel expression provides a powerful tool for future studies of mechanisms of regulation of ion channel expression.

The authors gratefully acknowledge a critique of the manuscript by Leslie C. McKinney, and the technical assistance of Donald R. Anderson. Carol A. Vandenberg (University of California at Santa Barbara) generously provided prepublication HH-IRK1 primer sequences. This project was supported by a Grant-in-Aid from the American Heart Association and National Institutes of Health grant R01-HL52671 to T.E. DeCoursey, by the Division of Pulmonary Medicine at Rush Presbyterian St. Luke's Medical Center, and by Multiple Sclerosis Society grant RG 2124-B-2/1 to F.N. Quandt.

## References

Altschul, S.F., Gish, W., Miller, W., Myers, E.W., Lipman, D.J. 1990. Basic local alignment search tool. *J. Mol. Biol.* **215**:403–410

Arcari, P., Martinelli, R., Salvatore, F. 1989. Human glyceraldehyde-3-phosphate dehydrogenase pseudogenes: molecular evolution and a possible mechanism for amplification. *Biochem. Genet.* **27**:439–450

Arkett, S.A., Dixon, S.J., Sims, S.M. 1992. Substrate influences rat osteoclast morphology and expression of potassium conductances. *J. Physiol.* **458**:633–653

Auwerx, J. 1991. The human leukemia cell line, THP-1: a multifaceted model for the study of monocyte-macrophage differentiation. *Experientia* **47**:22–31

Biermans, G., Vereecke, J., Carmeliet, E. 1987. The mechanism of the inactivation of the inward-rectifying K current during hyperpolarizing steps in guinea-pig ventricular myocytes. *Pfluegers Arch.* **410**:604–613

Buisman, H.P., Steinberg, T.H., Fischbarg, J., Silverstein, S.C., Vogelzang, S.A., Ince, C., Ypey, D.L., Leijh, P.C.J. 1988. Extracellular ATP induces a large nonselective conductance in macrophage plasma membranes. *Proc. Natl. Acad. Sci. USA* **85**: 7988–7992

Cahalan, M.D., Chandy, K.G., DeCoursey, T.E., Gupta, S. 1985. A voltage-gated potassium channel in human T lymphocytes. *J. Physiol.* **358**:197–237

Cahalan, M.D., Lewis, R.S. 1988. Role of potassium and chloride channels in volume regulation by T lymphocytes. In: *Cell Physiology of Blood*. R.B. Gunn and J.C. Parker, editors. pp. 281–301. Rockefeller University Press, New York

Cai, Y.-C., Osborne, P.B., North, R.A., Dooley, D.C., Douglass, J. 1992. Characterization and functional expression of genomic DNA encoding the human lymphocyte type n potassium channel. *DNA and Cell Biology* **11**:163–172

Chiu, S.Y., Wilson, G.F. 1989. The role of potassium channels in Schwann cell proliferation in Wallerian degeneration of explant rabbit sciatic nerves. *J. Physiol.* **408**:199–222

Chomczynski, P. 1993. A reagent for the single-step simultaneous isolation of RNA, DNA and proteins from cell and tissue samples. *Biotechniques* **15**:532–537

Colquhoun, D., Hawkes, A.G. 1985. The principles of the stochastic interpretation of ion-channel mechanisms. Chap. 9, pp. 135–175. In: *Single-Channel Recording*. B. Sakmann and E. Neher, editors. Plenum Press, New York

Conrad, G.W., Rink, T.J. 1986. Platelet activating factor raises intracellular calcium ion concentration in macrophages. *J. Cell Biol.* **103**:439–450

DeCoursey, T.E., Chandy, K.G., Gupta, S., Cahalan, M.D. 1984. Voltage-gated K<sup>+</sup> channels in human T lymphocytes: a role in mitogenesis? *Nature* **307**:465–468

DeCoursey, T.E., Chandy, K.G., Gupta, S., Cahalan, M.D. 1985. Voltage-dependent ion channels in T-lymphocytes. *J. Neuroimmunol.* **10**:71–95

DeCoursey, T.E., Chandy, K.G., Gupta, S., Cahalan, M.D. 1987. Mitogen induction of ion channels in murine T lymphocytes. *J. Gen. Physiol.* **89**:405–420

DeCoursey, T.E., Cherny, V.V. 1996. Voltage-activated proton currents in human THP-1 monocytes. *J. Membrane Biol.* **152**:2

Deutsch, C., Chen, L.-Q. 1993. Heterologous expression of specific K<sup>+</sup> channels in T lymphocytes: functional consequences for volume regulation. *Proc. Natl. Acad. Sci. USA* **90**:10036–10040

Deutsch, C., Krause, D., Lee, S.C. 1989. Voltage-gated potassium conductance in human T lymphocytes stimulated with phorbol ester. *J. Physiol.* **372**:405–423

Deutsch, C., Lee, S.C. 1988. Cell volume regulation in lymphocytes. *Renal Physiol. Biochem.* **3–5**:260–276

Di Virgilio, F., Meyer, B.C., Greenberg, S., Silverstein, S.C. 1988. Fc receptor-mediated phagocytosis occurs in macrophages at exceedingly low cytosolic Ca<sup>2+</sup> levels. *J. Cell Biol.* **106**:657–666

Douglass, J., Osborne, P.B., Cai, Y.-C., Wilkinson, M., Christie, M.J., Adelman, J.P. 1990. Characterization and functional expression of a rat genomic DNA clone encoding a lymphocyte potassium channel. *J. Immunol.* **144**:4841–4850

Dubois, J.M., Rouzaire-Dubois, B. 1993. Role of potassium channels in mitogenesis. *Prog. Biophys. Molec. Biol.* **59**:1–21

Ercolani, L., Florence, B., Denaro, M., Alexander, M. 1988. Isolation and complete sequence of a functional human glyceraldehyde-3-phosphate dehydrogenase gene. *J. Biol. Chem.* **263**:15335–15341

Fakler, B., Brändle, U., Bond, C., Glowatzki, E., König, C., Adelman, J.P., Zenner, H.-P., Ruppertsberg, J.P. 1994. A structural determinant of differential sensitivity of cloned inward rectifier K<sup>+</sup> channels to intracellular spermine. *FEBS Lett.* **356**:199–203

Gallin, E.K. 1984. Calcium and voltage activated potassium channels in human macrophages. *Biophys. J.* **46**:821–825

Gallin, E.K. 1989. Evidence for a Ca-activated inwardly rectifying K channel in human macrophages. *Am. J. Physiol.* **257**:C77–C85

Gallin, E.K. 1991. Ion channels in leukocytes. *Physiol. Rev.* **71**:775–811

Gallin, E.K., Livengood, D.R. 1981. Inward rectification in mouse macrophages: evidence for a negative resistance region. *Am. J. Physiol.* **241**:C9–C17

Gallin, E.K., Mason, T.M., Moran, A. 1994. Characterization of regulatory volume decrease in the THP-1 and HL-60 human myelocytic cell lines. *J. Cell. Physiol.* **159**:573–581

Gallin, E.K., McKinney, L.C. 1988. Patch-clamp studies in human macrophages: single-channel and whole-cell characterization of two K<sup>+</sup> conductances. *J. Membrane Biol.* **103**:55–60

Gallin, E.K., Sheehy, P.A. 1985. Differential expression of inward and outward potassium currents in the macrophage-like cell line J774.1. *J. Physiol.* **369**:475–499

Gallin, E.K., Wiederhold, M.L., Lipsky, P.E., Rosenthal, A.S. 1975. Spontaneous and induced membrane hyperpolarizations in macrophages. *J. Cell Physiol.* **86**:653–662

Gilliland, D.D., Perrin, S., Blanchard, K., Bunn, H.F. 1990. Analysis of cytokine mRNA and DNA: detection and quantification by competitive polymerase chain reaction. *Proc. Natl. Acad. Sci. USA* **87**:2725–2729

Grissmer, S., Dethlefs, B., Wasmuth, J.J., Goldin, A.L., Gutman, G.A., Cahalan, M.D., Chandy, K.G. 1990. Expression and chromosomal localization of a lymphocyte K<sup>+</sup> channel gene. *Proc. Natl. Acad. Sci. USA* **87**:9411–9415

Grissmer, S., Nguyen, A.N., Cahalan, M.D. 1993. Calcium-activated potassium channels in resting and activated human T lymphocytes: expression levels, calcium dependence, ion selectivity, and pharmacology. *J. Gen. Physiol.* **102**:601–630

Hara, N., Ichinose, M., Sawada, M., Imai, K., Maeno, T. 1990. Activation of single Ca<sup>2+</sup>-dependent K<sup>+</sup> channel by external ATP in mouse macrophages. *FEBS Lett.* **267**:281–284

Harvey, R.D., Ten Eick, R.E. 1989. Voltage-dependent block of cardiac inward-rectifying potassium current by monovalent cations. *J. Gen. Physiol.* **94**:349–361

Hass, R. 1992. Retrodifferentiation—an alternative biological pathway in human leukemia cells. *Eur. J. Cell Biol.* **58**:1–11

Hass, R., Giese, G., Meyer, G., Hartmann, A., Dörk, T., Köhler, L., Resch, K., Traub, P., Goppelt-Strübe, M. 1990. Differentiation and retrodifferentiation of U937 cells: reversible induction and suppression of intermediate filament protein synthesis. *Eur. J. Cell Biol.* **51**:265–271

Hutter, O.F., Williams, T.L. 1979. A dual effect of formaldehyde on the inwardly rectifying potassium conductance in skeletal muscle. *J. Physiol.* **286**:591–606

Kelly, M.E.M., Dixon, S.J., Sims, S.M. 1992. Inwardly rectifying potassium current in rabbit osteoclasts: a whole-cell and single-channel study. *J. Membrane Biol.* **126**:171–181

Kettenmann, H., Banati, R., Walz, W. 1993. Electrophysiological behavior of microglia. *Glia* **7**:93–101

Kettenmann, H., Hoppe, D., Gottmann, K., Banati, R., Kreutzberg, G. 1990. Cultured microglial cells have a distinct pattern of membrane channels different from peritoneal macrophages. *J. Neurosci. Res.* **26**:278–287

Kim, S.Y., Silver, M.R., DeCoursey, T.E. 1996. Ion channels in human THP-1 monocytes. *J. Membrane Biol.* **152**:2

Kubo, Y., Baldwin, T.J., Jan, Y.N., Jan, L.Y. 1993. Primary structure and functional expression of a mouse inward rectifier potassium channel. *Nature* **362**:127–133

Leonard, R.J., Garcia, M.L., Slaughter, R.S., Reuben, J.P. 1992. Selective blockers of voltage-gated K<sup>+</sup> channels depolarize human T lymphocytes: mechanism of the antiproliferative effect of charybdotoxin. *Proc. Natl. Acad. Sci. USA* **89**:10094–10098

Lewis, R.S., Cahalan, M.D. 1989. Mitogen-induced oscillations of cytosolic Ca<sup>2+</sup> and transmembrane Ca<sup>2+</sup> current in human leukemic T cells. *Cell Regulation* **1**:99–112

Lopatin, A.N., Makhina, E.N., Nichols, C.G. 1994. Potassium channel block by cytoplasmic polyamines as the mechanism of intrinsic rectification. *Nature* **372**:366–369

Lu, L., Yang, T., Markakis, D., Guggino, W.B., Craig, R.W. 1993. Alterations in a voltage-gated K<sup>+</sup> current during the differentiation of ML-1 human myeloblastic leukemia cells. *J. Membrane Biol.* **132**:267–274

Mahaut-Smith, M.P., Mason, M.J. 1991. Ca<sup>2+</sup>-activated K<sup>+</sup> channels in rat thymic lymphocytes: activation by concanavalin A. *J. Physiol.* **439**:513–528

Mahaut-Smith, M.P., Rink, T.J., Collins, S.C., Sage, S.O. 1990. Voltage-gated potassium channels and the control of membrane potential in human platelets. *J. Physiol.* **428**:723–735

Marty, A. 1983. Blocking of large unitary calcium-dependent potassium currents by internal sodium ions. *Pfluegers Arch.* **396**:179–181

Matsuda, H., Saigusa, A., Irisawa, H. 1987. Ohmic conductance through the inwardly rectifying K channel and blocking by internal Mg<sup>2+</sup>. *Nature* **325**:156–159

McKinney, L.C., Gallin, E.K. 1988. Inwardly rectifying whole-cell and single-channel K currents in the murine macrophage cell line J774.1. *J. Membrane Biol.* **103**:41–53

McKinney, L.C., Gallin, E.K. 1990. Effect of adherence, cell morphology, and lipopolysaccharide on potassium conductance and passive membrane properties of murine macrophage J774.1 cells. *J. Membrane Biol.* **116**:47–56

Nelson, D.J., Jow, B., Jow, F. 1990a. Whole cell currents in macrophages: I. Human monocyte-derived macrophages. *J. Membrane Biol.* **117**:29–44

Nelson, D.J., Jow, B., Jow, F. 1992. Lipopolysaccharide induction of outward potassium current expression in human monocyte-derived macrophages: lack of correlation with secretion. *J. Membrane Biol.* **125**:207–218

Nelson, D.J., Jow, B., Popovich, K.J. 1990b. Whole cell currents in macrophages: II. Alveolar macrophages. *J. Membrane Biol.* **117**:45–55

Nilius, B., Wohlrab, W. 1992. Potassium channels and regulation of proliferation of human melanoma cells. *J. Physiol.* **445**:537–548

Nörenberg, W., Appel, K., Bauer, J., Gebicke-Haerter, P.J., Illes, P. 1993. Expression of an outwardly rectifying K<sup>+</sup> channel in rat microglia cultivated on teflon. *Neurosci. Lett.* **160**:69–72

Nörenberg, W., Gebicke-Haerter, P.J., Illes, P. 1992. Inflammatory stimuli induce a new K<sup>+</sup> outward current in cultured rat microglia. *Neurosci. Lett.* **147**:171–174

Ohmori, H. 1978. Inactivation kinetics and steady-state current noise in the anomalous rectifier of tunicate egg cell membrane. *J. Physiol.* **281**:77–99

Pappone, P.A., Ortiz-Miranda, S.I. 1993. Blockers of voltage-gated K channels inhibit proliferation of cultured brown fat cells. *Am. J. Physiol.* **264**:C1014–C1019

Peters-Golden, M., McNish, R.W., Brieland, J.K., Fantone, J.C. 1990. Diminished protein kinase C-activated arachidonate metabolism accompanies rat macrophage differentiation in the lung. *J. Immunol.* **144**:4320–4326

Price, M., Lee, S.C., Deutsch, C. 1989. Charybdotoxin inhibits proliferation and interleukin 2 production in human peripheral blood lymphocytes. *Proc. Natl. Acad. Sci. USA* **86**:10171–10175

Raab-Graham, K.F., Radeke, C.M., Vandenberg, C.A. 1994. Molecular cloning and expression of a human heart inward rectifier potassium channel. *NeuroReport* **5**:2501–2505

Randriamampita, C., Trautmann, A. 1987. Ionic channels in murine macrophages. *J. Cell Biol.* **105**:761–769

Ravesloot, J.H., van Houten, R.J., Ypey, D.L., Nijweide, P.J. 1990. Identification of Ca<sup>2+</sup>-activated K<sup>+</sup> channels in cells of embryonic chick osteoblast cultures. *J. Bone Mineral Res.* **5**:1201–1210

Rouzaire-Dubois, B., Dubois, J.M. 1991. A quantitative analysis of the role of K<sup>+</sup> channels in mitogenesis of neuroblastoma cells. *Cell. Signal.* **3**:333–339

Rudy, B. 1988. Diversity and ubiquity of K channels. *Neurosci.* **25**:729–749

Silver, M.R., DeCoursey, T.E. 1990. Intrinsic gating of inward rectifier in bovine pulmonary artery endothelial cells in the presence or absence of internal Mg<sup>2+</sup>. *J. Gen. Physiol.* **96**:109–133

Silver, M.R., Shapiro, M.S., DeCoursey, T.E. 1994. Effects of external Rb<sup>+</sup> on inward rectifier K<sup>+</sup> channels of bovine pulmonary artery endothelial cells. *J. Gen. Physiol.* **103**:519–548

Sozzani, S., Molino, M., Locati, M., Luini, W., Cerletti, C., Vecchi, A., Mantovani, A. 1993. Receptor-activated calcium influx in human monocytes exposed to monocyte chemoattractant protein-1 and related cytokines. *J. Immunol.* **150**:1544–1553

Standen, N.B., Stanfield, P.R. 1979. Potassium depletion and sodium block of potassium currents under hyperpolarization in frog skeletal muscle. *J. Physiol.* **294**:497–520

Standen, N.B., Stanfield, P.R. 1980. Rubidium block and rubidium permeability of the inward rectifier of frog skeletal muscle. *J. Physiol.* **304**:415–435

Stickle, D.F., Daniele, R.P., Holian, A. 1984. Cytosolic calcium, calcium fluxes, and regulation of alveolar macrophage superoxide anion production. *J. Cell. Physiol.* **121**:458–466

Sung, S.-S.J., Young, J.D.-E., Origlio, A.M., Heiple, J.M., Kaback, H.R., Silverstein, S.C. 1985. Extracellular ATP perturbs transmembrane ion fluxes, elevates cytosolic [Ca<sup>2+</sup>], and inhibits phagocytosis in mouse macrophages. *J. Biol. Chem.* **260**:13442–13449

Teulon, J., Ronco, P.M., Geniteau-Legendre, M., Baudouin, B., Estrade, S., Cassingena, R., Vandewalle, A. 1992. Transformation of renal tubule epithelial cells by simian virus 40 is associated with emergence of Ca<sup>2+</sup>-insensitive K<sup>+</sup> channels and altered mitogenic sensitivity to K<sup>+</sup> channel blockers. *J. Cell. Physiol.* **151**:113–125

Verheugen, J.A.H., Vijverberg, H.P.M., Oortgiesen, M., Cahalan, M.D. 1995. Voltage-gated and Ca<sup>2+</sup>-activated K<sup>+</sup> channels in intact hu-

man T lymphocytes: noninvasive measurements of membrane currents, membrane potential, and intracellular calcium. *J. Gen. Physiol.* **105**:765–794

Weidema, A.F., Ravesloot, J.H., Panyi, G., Nijweide, P.J., Ypey, D.L. 1993. A  $\text{Ca}^{2+}$ -dependent  $\text{K}^+$  channel in freshly isolated and cultured chick osteoclasts. *Biochim. Biophys. Acta* **1149**:63–72

Wieland, S.J., Cho, R.H., Gong, Q-H. 1990. Macrophage-colony-stimulating factor (CSF-1) modulates a differentiation-specific inward-rectifying potassium current in human leukemic (HL-60) cells. *J. Cell. Physiol.* **142**:643–651

Wieland, S.J., Gong, Q-H., Chou, R.H., Brent, L.H. 1992. A lineage-specific  $\text{Ca}^{2+}$ -activated  $\text{K}^+$  conductance in HL-60 cells. *J. Biol. Chem.* **267**:15426–15431

Yellen, G. 1984. Ionic permeation and blockade in  $\text{Ca}^{2+}$ -activated  $\text{K}^+$  channels of bovine chromaffin cells. *J. Gen. Physiol.* **84**:157–186

Young, J.D-E., Ko, S.S., Cohn, Z.A. 1984. The increase in intracellular free calcium associated with IgG $\gamma$ 2b/ $\gamma$ 1 Fc receptor-ligand interactions: role in phagocytosis. *Proc. Natl. Acad. Sci. USA* **81**:5430–5434

Ypey, D.L., Clapham, D.E. 1984. Development of a delayed outward-rectifying  $\text{K}^+$  conductance in cultured mouse peritoneal macrophages. *Proc. Natl. Acad. Sci. USA* **81**:3080–3087